Formaldehyde-responsive proteins, TtmR and EfgA, reveal a tradeoff between formaldehyde resistance and efficient transition to methylotrophy in *Methylorubrum extorquens*

Jannell V. Bazurto[1,2,3,4,5,6], Eric L. Bruger[1,2,3], Jessica A. Lee[1,2,3,7], Leah B. Lambert[1], and Christopher J. Marx[1,2,3].

Running title:

TtmR and EfgA role in the transition to methylotrophy

Keywords:

Methylotrophy, formaldehyde, stress response, adaptation, tradeoffs, Enhanced formaldehyde growth protein A (EfgA), MarR transcription factor

Affiliations:

[1]Department of Biological Sciences, University of Idaho, Moscow, ID

[2]Insititute for Modeling Collaboration and Innovation, University of Idaho, Moscow, ID

[3]Institute for Bioinformatics and Evolutionary Studies, University of Idaho, Moscow, ID

[4]Department of Plant and Microbial Biology, University of Minnesota, Twin Cities, MN

[5]Microbial and Plant Genomics Institute, University of Minnesota, Twin Cities, MN

[6]Biotechnology Institute, University of Minnesota, Twin Cities, MN

[7]NASA Ames Research Center, Moffett Field, CA

Contributions:

Jannell V. Bazurto: Conceptualization, funding acquisition, investigation, methodology, visualization, writing - original draft preparation, writing – review & editing

Eric L. Bruger: Conceptualization, funding acquisition, investigation, methodology, visualization, writing - original draft preparation, writing – review & editing

Jessica A. Lee: Conceptualization, investigation, methodology, writing - original draft preparation, writing – review & editing

Leah B. Lambert: Funding acquisition, investigation

Christopher J. Marx: Conceptualization, funding acquisition, project administration, resources, supervision, writing - original draft preparation, writing – review & editing

Acknowledgements:

We thank Juan E. Abrahante of the University of Minnesota Informatics Institute (UMII) for assistance with the pipeline for RNA-Seq data analysis and Siavash Riazi for assistance with modifying R scripts. We thank members of the Marx laboratory and Lon Chubiz for critical reading of this manuscript. The flow cytometry was carried out at the IBEST Optical Imaging

Core at the University of Idaho (IBEST is supported in part by NIH COBRE grant P30GM103324). This work was supported by funding from an Army Research Office MURI sub-award to CJM (W911NF-12-1-0390), a CMCI Pilot Grant to CJM (parent NIH award P20GM104420), an INBRE Undergraduate Research Fellowship to LBL (parent NIH award P20GM103408), and a BEACON Center for Evolution in Action Pilot Grants to JVB and ELB (NSF Cooperative Agreement DBI-0939454).

ABSTRACT

For bacteria to thrive they must be well-adapted to their environmental niche, which may involve specialized metabolism, timely adaptation to shifting environments, and/or the ability to mitigate numerous stressors. These attributes are highly dependent on cellular machinery that can sense both the external and intracellular environment. *Methylorubrum extorquens* is an extensively studied facultative methylotroph, an organism that can use single-carbon compounds as their sole source of carbon and energy. In methylotrophic metabolism, carbon flows through formaldehyde as a central metabolite; thus, formaldehyde is both an obligate metabolite and a metabolic stressor. Via the one-carbon dissimilation pathway, free formaldehyde is rapidly incorporated by formaldehyde activating enzyme (Fae), which is constitutively expressed at high levels. In the presence of elevated formaldehyde levels, a recently identified formaldehyde-sensing protein, EfgA, induces growth arrest. Herein, we describe TtmR, a formaldehyde-responsive transcription factor that, like EfgA, modulates formaldehyde resistance. TtmR is a member of the MarR family of transcription factors and impacts the expression of 75 genes distributed throughout the genome, many of which are transcription factors and/or involved in stress response, including *efgA*. Notably, when *M. extorquens* is adapting its metabolic network during the transition to methylotrophy, *efgA* and *ttmR* mutants experience an imbalance in formaldehyde production and a notable growth delay. Although methylotrophy necessitates that *M. extorquens* maintain a relatively high level of formaldehyde tolerance, this work reveals a tradeoff between formaldehyde resistance and the efficient transition to methylotrophic growth and suggests that TtmR and EfgA play a pivotal role in maintaining this balance.

Importance: All organisms produce formaldehyde as a byproduct of enzymatic reactions and as a degradation product of metabolites. The ubiquity of formaldehyde in cellular biology suggests all organisms have evolved mechanisms of mitigating formaldehyde toxicity. However, formaldehyde-sensing is poorly described and prevention of formaldehyde-induced damage is primarily understood in the context of detoxification. Here we use an organism that is regularly exposed to elevated intracellular formaldehyde concentrations through high-flux one-carbon utilization pathways to gain insight into the role of formaldehyde-responsive proteins that modulate formaldehyde resistance. Using a combination of genetic and transcriptomic analyses, we identify dozens of genes putatively involved in formaldehyde resistance, determined the relationship between two different formaldehyde response systems and identified an inherent tradeoff between formaldehyde resistance and optimal transition to methylotrophic metabolism.

INTRODUCTION

Methylotrophy, a trait found in all domains of life, is the unique metabolic ability of organisms to use one- or multi-carbon compounds lacking carbon-carbon bonds, as sole sources of carbon and energy. Growth substrates for methylotrophs include compounds such as methane (methanotrophs), methanol, and methylamines (mono-, di-, tri-), and methylated sulfur species. A key feature of methylotrophic metabolism is that each carbon of the growth substrate flows through the potent toxin formaldehyde as a central intermediate. Formaldehyde is harmful to all cell types because of its reactivity with electrophiles such as free amines and thiols. It can form adducts with or crosslink a number of biological molecules such as DNA and proteins. Despite the centrality of formaldehyde in methylotrophic metabolism, until very recently formaldehyde-specific stress responses had not been described in methylotrophs.

In *Methylorubrum* (formerly *Methylobacterium*) *extorquens* AM1 the most extensively studied facultative methylotroph, the intracellular formaldehyde concentration is estimated at ~ 1 mM during growth on methanol (1). Methanol is directly oxidized to formaldehyde in the periplasm by methanol dehydrogenase (MDH). Free endogenous formaldehyde is kept relatively low in the cytoplasm by formaldehyde activating enzyme (Fae), which condenses formaldehyde with the C_1 carrier dephosphotetrahydromethanopterin (dH_4MPT); this is the first of three reactions in the pterin-dependent dissimilatory pathway that oxidizes formaldehyde to formate (2–4). Previous work has demonstrated that strains defective in formaldehyde dissimilation by disruption of pathway enzymes (*fae*) or synthesis of the dH_4MPT C_1 carrier (*mptG*) are sensitive to methanol (4). Formate is the branchpoint metabolite and can be further oxidized to CO_2 for energy production or shunted toward a tetrahydrofolate-dependent assimilation pathway for ultimate incorporation into biomass via the serine cycle (5, 6).

Very recently experimental evolution of *M. extorquens* PA1 for growth on formaldehyde as a sole source of carbon and energy revealed multiple loci that could increase formaldehyde resistance (7). Although dissimilation by the dH_4MPT pathway is the primary mechanism for removing free formaldehyde from the cytoplasm (3, 4), none of the beneficial mutations were in these genes. Instead, this work found that single mutations in one of three genetic loci (*efgA, def, Mext_0925*) could independently confer the ability to use formaldehyde as a sole source of carbon and energy. The most frequent class of mutations (nearly 80%) were loss-of-function mutations in **e**nhanced **f**ormaldehyde **g**rowth protein **A** (EfgA), a protein that directly binds formaldehyde and halts translation in the presence of excess formaldehyde by an unknown mechanism. Though strains lacking EfgA can grow in the presence of higher formaldehyde concentrations than wild-type, the absence of EfgA increases methanol sensitivity in strains that are vulnerable to formaldehyde stress (*fae*, *mptG*), suggesting that the physiological role of EfgA is to decrease formaldehyde-induced stress. Peptide deformylase (PDF, encoded by *def)*, is a ribosomally-associated enzyme that is essential for translation and involved in protein quality control (8). Selection for mutations in *def,* provided further evidence for the importance of translational regulation in response to formaldehyde stress.

Mext_0925 is a homolog of the MarR transcription factor (7). This family of regulators is found in bacteria and archaea and was originally characterized in *Escherichia coli* (9–12). In *E. coli*, MarR is encoded by the multiple antibiotic resistance (*mar*) operon. It is a ligand-sensing repressor that binds the operator of the *marRAB* operon in the absence of ligand and is thus self-regulating (13, 14). A number of structurally distinct compounds such as tetracycline, chloramphenicol, and salicylate can bind MarR and induce conformational changes that lead to DNA release (19). Additionally, the *marRAB* operon can be activated by aromatic amino acid metabolites directly

and indirectly (15). Subsequently, *marRAB* expression gives rise to the transcription factor MarA, a member of the AraC/XylS family, which in turn upregulates dozens of genes that contribute to resistance to multiple antibiotics, oxidative stress, and organic solvent stress (16–18). Broader examination of MarR homologs in a variety of organisms show that homologs i) can be repressors, activators, or both, ii) have highly variable regulon sizes, and iii) control a variety of cellular processes involved in various stress responses and metabolic pathways (19).

In *Bacillus subtilis*, the MarR homolog HxlR has a role in formaldehyde stress response (20, 21). *hxlR* is divergently transcribed from the *hxlAB* operon that HxlR positively regulates. The *hxlAB* operon encodes two key proteins of the ribulose monophosphate pathway of formaldehyde detoxification and is induced by exogenous formaldehyde (20, 22). *In vitro*, formaldehyde does not impact binding of HxlR and, as is the case with several MarR homologs, the mechanism of activation has remained elusive. In some instances, however, the mechanism of activation of MarR homologs is clear. For example, in organisms such as *Acinetobacter baylyi* and *Streptomyces coelicolor*, where MarR homologs regulate operons encoding enzymes required for the catabolism of aromatic lignin-derivatives such as ferulate and protocatechuate, respectively, ligand binding leads to release of cognate DNA and the operon is derepressed (19, 23–25). This leads to expression of the relevant enzymes and the ligand/carbon substrates are utilized.

Herein, we probe the physiological role of Mext_0925, implicated in modulating formaldehyde resistance. Unlike many described MarR homologs, *Mext_0925* is not in an operon or divergently transcribed from an operon, thus there is no genomic context for discerning its regulon. In the absence of obvious genetic associations, we opted to use transcriptomic analyses to identify differentially expressed genes in a Δ*Mext_0925* mutant. By coupling this approach with *in vivo* genetic studies, we find that Mext_0925 is specifically responsive to formaldehyde stress. Our

159 results define the relationship between Mext_0925 and EfgA, the only characterized formaldehyde
160 stress response system in *M. extorquens*, and demonstrate that the ability of *M. extorquens* to
161 respond to formaldehyde stress at the transcriptional and translational levels is critical for the
162 optimal transition to methylotrophy. Based on our findings, we conclude that Mext_0925
163 represents a second formaldehyde-specific response system in *M. extorquens* and suggest the name
164 TtmR, for a regulator of the **t**ransition **t**o **m**ethylotrophy.

165

MATERIALS AND METHODS

Bacterial strains, media, and chemicals

Bacterial strains used in this study (Table S1) are derivatives of *Methylorubrum extorquens* PA1 (formerly *Methylobacterium*) (26–28) where genes for cellulose synthesis were deleted to prevent aggregation and optimize liquid growth measurements (29). Therefore, the genotype referred to herein as 'wild-type' (CM2730) is more accurately Δ*celABC*. The Δ*efgA* mutant (CM3745) additionally has a markerless deletion that eliminated 404 bp from the ORF of *Mext_4158* (21-424/435 bp) (7) and the Δ*ttmR* mutant (CM4732) has a markerless deletion of the entire coding region (588 bp) of *Mext_0925*. All growth experiments with liquid medium were performed with *Methylobacterium* PIPES (MP) medium (29) with 3.5 mM succinate, 15 mM methanol, or 2, 4, 6, 8, 10 mM formaldehyde as a carbon source. For growth on solid MP medium, Bacto Agar (15 g/L, BD Diagnostics) was added and carbon source concentrations were elevated (15 mM succinate, 125 mM methanol). Formaldehyde stock solutions (1 M) were prepared by boiling a mixture of 0.3 g paraformaldehyde and 10 mL of 0.05 N NaOH in a sealed tube for 20 min; stock solutions were kept at room temperature and made fresh weekly. When present in the media, kanamycin was used at a final concentration of 50 μg/mL.

Genetic approaches

Markerless deletions were generated by allelic exchange as previously described using either pCM433 (30) or pPS04 (7). Vectors were designed using SnapGene software. The HiFi assembly kit from New England Biolabs was used to construct vectors from linearized vector backbone (restriction enzyme-digested) and PCR-generated inserts.

187

188 **Growth quantitation**

189 To initiate liquid growth, individual colonies were used to inoculate 2 mL MP medium containing
190 3.5 mM succinate or 15 mM methanol in biological triplicate. Cultures were shaken (250 rpm)
191 during incubation at 30 °C for 24 hr (succinate) or 36 hr (methanol) and then subcultured (1/64)
192 into 5 mL of identical medium for further acclimation. After this second 24-36 hr (succinate) or
193 36-48 hr (methanol) incubation, the stationary phase acclimation cultures were again subcultured
194 (1/64) into relevant media for growth measurements. Cell density was determined by monitoring
195 absorbance with a Spectronic 200 (Thermo Scientific) or a SmartSpec Plus (Bio-Rad) at 600 nm.
196 Final yield is defined as the absorbance reached upon entry into stationary phase. Cell viability
197 was determined by harvesting cells from a 100 µL aliquot of culture by centrifugation, discarding
198 supernatant and resuspending the cell pellet into an equal volume of MP medium (no carbon). Cell
199 suspensions were then serially diluted (1/10 dilutions, 200 µL total volume) in 96 well polystyrene
200 plates with MP medium (no carbon) and 10 µL aliquots of each dilution were spotted to MP
201 medium plates (15 mM succinate) using technical triplicates. Plates were inverted and incubated
202 at 30 °C until colony formation was apparent (4-6 d) at which point colonies were counted.
203 Technical triplicates were averaged for each sample; biological replicates were averaged.

204 **Formaldehyde quantification**

205 Formaldehyde concentrations in the culture media were measured as previously described (31).
206 Supernatant from a 100 µL aliquot of culture was isolated by centrifugation (14,000 x g). In
207 technical triplicate, 10 µL of the supernatant or 100 µL of 0.1X supernatant (diluted with MP
208 medium, no carbon) was combined with 190 or 100 µL Nash reagent B (2 M ammonium acetate,

50 mM glacial acetic acid, 20 mM acetylacetone), respectively, in 96 well polystyrene plates. Reaction plates were incubated (60 °C, 10 min), cooled to room temp (5 min), and absorbance was read at 432 nm on a Wallac 1420 VICTOR Multilabel reader (Perkin Elmer). Formaldehyde standards were prepared daily from 1 M formaldehyde stock solutions and a standard curve was read alongside all sample measurements.

RNA-Sequencing analysis

The WT (CM2730) and the Δ*ttmR* mutant (CM4732) were grown in biological triplicate in MP medium with 15 mM methanol as described above. The final growth vessel was a 250 mL flask, with a culture volume of 100 mL. When OD_{600} reached 0.2-0.3, cells from 50 mL of culture were harvested by centrifugation in an Eppendorf Centrifuge 5810R (5 min, 4,000xg, 4 °C). The supernatant was decanted and cells were washed with ice cold MP medium (no carbon) and centrifuged once more to remove wash supernatant. Pellets were immediately frozen by submerging tubes in liquid nitrogen and stored at -80 °C.

Nucleic acid extraction and molecular manipulation (RNA extraction, cDNA generation, library preparation) and sequencing were conducted by Genewiz (South Plainfield, NJ). The total RNA was extracted with the RNeasy Plus Mini Kit (Qiagen); rRNA was depleted with the Ribo-Zero rRNA removal kit (Illumina); the quality of resulting RNA samples was determined with an Agilent 2100 BioAnalyzer and Qubit assay. Once the cDNA library was generated, it was sequenced on an Illumina HiSeq (2x150 bp). The raw data (FASTQ format) was provided to investigators for further analysis.

An analysis pipeline developed by the University of Minnesota Genomics Center and the Research Informatics Solutions (RIS) group at the University of Minnesota Supercomputing Institute was

used for data analysis. The pipeline uses FastQC (32) to assess the quality of the sequencing data, Trimmomatic (33) to remove the low quality bases and adapter sequences, HISAT2 (34) to align the curated reads to the *M. extorquens* PA1 genome [GenBank accession: CP000908.1], Cuffquant and Cufnorm from the Cufflinks package (35) to generate FPKM expression values, and featureCounts from the Rsubread R package (36) to generate raw read counts. DESeq2 was used to convert raw count data to normalized counts and all further statistical analyses were carried out in R (37). Differentially expressed genes in the Δ*ttmR* mutant were identified by a pair-wise comparison to the WT strain and had a $\log_2$ fold change > 1 and a False Discovery Rate (FDR) adjusted p-value < 0.05.

Stress tests

For all tests, cultures of WT (CM2730) and the *ttmR*^{EVO} mutant (CM3919) were grown in biological triplicate in MP medium (succinate), as described above.

Alternative aldehyde growth assays.

Growth was quantified in liquid media as described above with succinate or methanol as the primary carbon source. Wild-type (CM2730) was subjected to variable glyoxal, acetaldehyde, glutaraldehyde, butyraldehyde, and propionaldehyde (up to 10 mM) to identify a concentration that would lead to a growth defect but allow growth within a 24 hr period. Once the working concentrations were identified (1.25 mM for acetaldehyde and glyoxal, 2.5 mM for the remaining aldehydes), the *ttmR*^{EVO} (CM3919) and Δ*efgA* (CM3745) mutants were grown in identical conditions, alongside the wild-type control.

Antibiotic resistance assays.

Stationary phase cultures (100 µL) in MP medium (succinate) were used to inoculate 3.5 mL of soft agar (0.8%) that was previously melted and then cooled to ~ 50 °C. Inoculated soft agar was agitated by vortex (~ 10 sec) and then overlaid to solid MP medium (succinate). Soft agar overlays were allowed to solidify at room temperature for 1-2 hr. Antibiotic discs (VWR) saturated with absolute amounts of individual antibiotics (novobiocin (5 µg), tetracycline (30 µg), streptomycin (10 µg), chloramphenicol (30 µg), colistin (10 µg), cefoxitin (30 µg), gentamycin (10 µg), erythromycin (15 µg), rifampicin (5 µg), ciprofloxacin (10 µg), vancomycin (30 µg), kanamycin (30 µg), nalidixic acid (30 µg), ampicillin (10 µg)) were placed on top of agar plates with sterile tweezers. Plates were incubated at 30 °C for ~ 24 hr and then scored for diameter of resulting zones of inhibition.

Oxidative stress.

Stationary phase cultures were used to prepare soft agar overlays as described for antibiotic resistance assays. After solidification, 5 µL of 30 % hydrogen peroxide (38) was spotted to the center of the plate (38). Plates were incubated at 30 °C for 4-6 d and scored for diameter of resulting zones of inhibition.

Alcohol stress.

Stationary phase cultures were serially diluted with MP medium (no carbon), plated to solid medium containing 2% ethanol (38) and incubated at 30 °C for 4-6 d and scored for indication of stress (colony size, small or variable) and viability.

Heat shock.

Mid-exponential phase cultures were placed in a 55 °C water bath for 5 or 10 min (38). Cells were then transferred to room temperature and serially diluted with MP medium (no growth carbon source) and plated to solid medium (succinate). After incubation at 30 °C for 4-6 d they were scored for viability (survival).

Assessing population heterogeneity

Isolated colonies were inoculated into 2 mL liquid MP media with either 3.5 mM succinate or 15 mM methanol. Upon growth, cultures were diluted 1/64 into 5 mL of the same liquid media in sealed Balch tubes and grown for 24 hr (succinate) or 30 hr (methanol) to allow all cultures to reach stationary phase. After completing this acclimation step, 1 mL of each culture was collected and centrifuged for 1 minute at 10,000xg. The supernatant was removed and the cell pellet was resuspended in 500 µL Diluent C containing 2 µL PKH67 dye (PKH67 Green Fluorescent Cell Linker Kit, Sigma-Aldrich), incubated for 5 minutes at room temperature, and quenched by adding 500 µL 1% BSA solution. Samples were pelleted for 1 minute at 10,000xg and subsequently washed in equal volumes of 1% BSA (once) followed by MP medium (twice). After a final resuspension in an equal volume of MP medium, the final mixes were diluted 1/64 into 5 mL MP media containing 15 mM methanol to initiate experimental cultures and the remainder was mixed with DMSO to 8% and stored at -80 °C. Samples taken during the experimental growth period were also mixed with DMSO to 8% and stored at -80 °C. Signal intensity of samples was assessed via flow cytometry analysis (Beckman Coulter Cytoflex S). After excitation at 488 nm, dye intensity was measured via emission detected with a 525 nm bandpass filter. Cell gating was determined by the distribution of red fluorescence detection from the mCherry-tagged strain CM3839.

RESULTS

Loss of a MarR-family regulator confers formaldehyde resistance.

To test whether the previously identified *ttmR*^{EVO} allele (ref 7) is a loss-of-function allele a precise deletion of the coding region *ttmR* was constructed by allelic exchange in wild-type and its growth was characterized. The one base-pair deletion in *ttmR*^{EVO} was in the open reading frame; the frameshift at 140/588 nt yielded a truncated protein with 73 amino acids, only 46 of which were wild-type. The evolved isolate with *ttmR*^{EVO} and the Δ*ttmR* strain could each use 4 mM formaldehyde as a sole carbon source, reaching a modest absorbance of ~ 0.10 - 0.13 when 4 mM formaldehyde was provided. At 6 mM formaldehyde, both the *ttmR*^{EVO} and Δ*ttmR* mutants failed to grow after 48 hr, unlike the Δ*efgA* strain (Figures 1A and 2A). Growth in the presence of 4 but not 6 mM formaldehyde was also seen when formaldehyde was added to an additional carbon source, either succinate or methanol (Figure 1BC). In the absence of exogenous formaldehyde (i.e., during growth on succinate or methanol alone), however, the Δ*ttmR* strain did not display any differences in lag time, growth rate, or final yield when compared to wild-type (Figure 2B, C, Table S2). Phenotypic comparison of *ttmR* and Δ*efgA* mutants demonstrate that although the Δ*efgA* mutant was more formaldehyde resistant, the mutations are comparable in that they i) allowed formaldehyde growth, ii) did not impact growth in the absence of formaldehyde stress, and ii) conferred formaldehyde resistance during the consumption of alternative carbon sources (Figures 1 and 2) (7).

TtmR is not involved in a general stress response.

The exact nature of formaldehyde cytotoxicity in *M. extorquens* is unknown; however, in various organisms, previous work has identified numerous forms of formaldehyde-induced DNA damage

316 (39, 40) and more recent work has implicated formaldehyde-induced protein damage in human
317 cell cytotoxicity (41). In considering possible mechanisms of increased formaldehyde resistance,
318 we recognized that cellular processes that are likely to mitigate formaldehyde-induced damage,
319 such as DNA repair and protein quality control, might be involved in generalized stress responses
320 or formaldehyde-specific stress responses. To address whether the loss of TtmR led to a
321 formaldehyde-specific response, the *ttmR*^{EVO} strain was exposed to a variety of other stressors.
322 Specifically, we chose stressors that addressed the possibilities that the *ttmR*^{EVO} mutant might i)
323 be broadly resistant to aldehydes, ii) confer multidrug resistance (as a homolog of MarR) or iii)
324 mediate a generalized stress response.

325 Growth assays in media supplemented with various C_2 aldehydes (glyoxal and acetaldehyde), as
326 well as a few other aldehydes (butyraldehyde, propionaldehyde, and glutaraldehyde) representing
327 potential metabolic intermediates indicated TtmR appears to be specific to formaldehyde stress. In
328 both succinate and methanol-based media, the *ttmR*^{EVO} mutant showed comparable defects in
329 growth to WT other than a very subtle growth improvement when either glyoxal or acetaldehyde
330 was present (Figure S1).

331 To evaluate antibiotic resistance, disk diffusion assays with different antibiotics were performed
332 with WT or Δ*ttmR* mutant soft agar overlays. Wild-type was resistant to 9 of the 14 antibiotics
333 tested (i.e., no zone of inhibition) (Table S3). Of the five remaining antibiotics, the Δ*ttmR* mutant
334 did not display any increased resistance (i.e., smaller zone), allowing us to conclude that though
335 there may be differences in specific antibiotic resistances, but there was no broadly acquired
336 antibiotic resistance (Table S3).

Finally, the *ttmR*^{EVO} strain was screened for its increased resistance to heat shock (55 ℃, treated 24 hr after entry into stationary phase in liquid medium), oxidative stress (H_2O_2, soft agar overlays), and alcohol stress (EtOH, in solid medium). The *ttmR*^{EVO} mutant strain behaved similar to wild-type when exposed to each of the stressors, other than a modest increase in viability during heat shock, which may indicate an elevated protein stress response (Table S3). Collectively, these data demonstrate that TtmR is not a general stress response protein but rather its activity is specific to modulating stress induced by formaldehyde.

TtmR modulates the expression of genes involved in an array of cellular functions.

To understand the impact of TtmR on the transcriptome, we performed RNA-sequencing analysis on wild-type and the Δ*ttmR* mutant during early exponential growth (OD = 0.2) in minimal medium with 15 mM methanol. Specifically, we aimed to identify differentially expressed genes (DEGs) that would explain the increased resistance to formaldehyde.

A pair-wise comparison of log-transformed counts of wild-type and the Δ*ttmR* mutant was performed and DEGs were identified by imposing a two-fold change cutoff ($Log_2FC > 1.0$) with an adjusted p-value (p_{adj}) less than 0.05. In total, we identified 75 DEGs in the Δ*ttmR* mutant, of which 61 (81%) were upregulated and 14 (19%) were downregulated (Tables 1, Figures 3 and S2). The expression differences observed in the upregulated genes were quite large; 34 had fold changes $\geq$4X ($Log_2FC>2.0$) and six had fold changes $\geq$10X ($Log_2FC\geq3.3$). By contrast, all downregulated genes had $\leq$4.6X fold change. Notably, several of the most upregulated DEGs (eg, 5 of the 6 with fold changes $\geq$10X) were clustered in the chromosome in operons or multiple adjacent operons (Figure 3).

Using their RefSeq annotations and Pfam domains, gene functionality of all of the DEGs were categorized into 14 groups which included 12 groups of genes with inferred functionality (n=58), one group that encoded hypothetical proteins (n=11), and one group of singletons (n=6), whose functionality was only represented by a single DEG (Figure S3). Of the 58 DEGs with a proposed function, the largest categories were Regulatory (n=12), Stress (n=10), Signaling (n=8), and Transport (n=7). Genes classified as Regulatory were comprised of a variety of transcription factors, sigma factors, or anti-sigma factors. Of the Regulatory DEGs, three were Crp homologs, predicted to bind cyclic nucleotides, and three were predicted to have roles in stress response (oxidative stress, cold shock, and generalized stress response, respectively). As many of the DEGs are themselves regulatory, the full array of DEGs identified in the Δ*ttmR* mutant likely represent loci that are directly controlled by TtmR and indirectly controlled by TtmR, through other regulators. The Signaling group included genes that encoded one or more PAS sensor domains and/or predicted members of two-component regulatory systems such as histidine kinases or response regulator receivers (single domain or paired with diguanylate cyclase domain). DEGs of the Stress group encoded universal stress proteins, whose mechanisms are highly variable, and proteins predicted to be involved in oxidative stress and solvent stress. Genes in the Transport grouping were involved in a Type I Secretion System (T1SS) and ABC transporters. There was little indication about the molecules that might be transported, with the exception of an annotated sulfonate transporter. The remaining DEGs were involved in Carbon metabolism, Cytochrome metabolism, C-N hydrolase and Chaperone/Heat shock.

The DEGs that were downregulated in the Δ*ttmR* mutant strain were scattered across functional categories with the exception of three of the four DEGs encoding Chaperonin/Heat shock proteins.

One possibility for the downregulated DEGs is that they are positively regulated by TtmR, when it is present.

Interestingly, we noticed inconsistency in the directionality of expression changes for Chaperone genes. Chaperonin GroEL, Chaperonin Cpn10, and Heat shock protein Hsp20 were downregulated while a second Heat shock protein Hsp20 homolog, *Mext_3498*, was significantly upregulated (14.5X, $Log_2FC=3.9$). *Mext_3498* was part of the highly upregulated twelve-gene cluster and appears to be the first gene in a two-gene operon that also encoded a Crp homolog with a cyclic nucleotide binding motif. These non-uniform changes may reflect the distinct roles of Chaperones involved in housekeeping protein quality control versus those which are stress-related. The considerable upregulation of Heat shock protein Hsp20 homolog, *Mext_3498*, may prevent formaldehyde-induced protein damage even in the midst of downregulation of Chaperonin GroEL, Chaperonin Cpn10, and a second homolog of Heat shock protein Hsp20.

Of the 75 DEGs identified herein, 20 of them were identified in the 33 previously associated with the transcriptome of the phenotypically formaldehyde-tolerant subpopulation of wild-type *M. extorquens* described elsewhere (42). We find that the directionalities, but not the magnitudes, of expression changes are comparable to those found in the formaldehyde-tolerant subpopulation (Figure 3, Table 1). In all 20 instances, gene expression differences were more pronounced in the Δ*ttmR* mutant than in the subpopulation. The genes of the methanol utilization pathways in the Δ*ttmR* mutant did not meet our conservative criteria for being identified as DEGs. However, closer examination showed modest decreases (~ 1.3-1.6 fold changes, p-adj < 0.05) in the expression of *mxaF,* which encodes the large subunit of methanol dehydrogenase (43, 44), as well as genes involved in formate assimilation and oxidation (Table S4).

Overall our data suggests that TtmR elimination allows formaldehyde resistance by tuning the expression of a number of loci that collectively launch a formaldehyde-specific physiological response that may include downstream regulation, cyclic nucleotide signaling, transport, and general stress responses. Notably, the DEGs identified were not involved in cellular functions most often associated with formaldehyde stress, such as DNA repair or formaldehyde detoxification by methylotrophic pathways or alcohol/aldehyde dehydrogenases.

TtmR can modulate formaldehyde resistance independent of EfgA.

EfgA is a predicted formaldehyde sensor that modulates formaldehyde resistance by halting translation in the presence of elevated formaldehyde (7). Like TtmR, the absence of EfgA confers *M. extorquens* with the ability to grow on formaldehyde as a sole source of carbon and energy (Figure 1A), presumably because formaldehyde-mediated translational pausing has been eliminated. Our transcriptomic analysis showed that *efgA* was ~ 2.0X downregulated in the Δ*ttmR* mutant. Thus, our data suggested it was possible that TtmR mediates formaldehyde resistance through regulating *efgA* expression.

To test this hypothesis, we constructed a Δ*ttmR* Δ*efgA* double mutant by successive allelic exchange. We then compared the growth of the double mutant to that of each of the single mutants with variable concentrations of formaldehyde provided in the media. In the absence of exogenous formaldehyde, growth of the double mutant was indistinguishable from either of the single mutants (data not shown). By contrast, when 6 mM formaldehyde was added to the growth medium, the Δ*ttmR* mutant failed to grow after 24 hr, while the Δ*ttmR* Δ*efgA* double mutant was more fit than the Δ*efgA* single mutant (Figure 4). These data demonstrated that TtmR has some effects that

extend beyond regulating EfgA, although the transcriptomic data suggest that the formaldehyde resistance of *ttmR* mutants might be partially mediated by decreased *efgA* expression.

TtmR and EfgA are required for optimal transition to methylotrophy.

To understand when TtmR and EfgA would be beneficial to *M. extorquens*, we sought to identify growth conditions that induced formaldehyde stress in a physiologically relevant context (i.e., from methanol utilization). Previous work has demonstrated that during the switch from multi-carbon to single-carbon growth, *M. extorquens* AM1 experiences a transient formaldehyde imbalance, such that formaldehyde is secreted into the growth medium (45). Researchers suggested that imbalance occurs as a result of non-transcriptional regulation preventing flux through methylotrophic pathways where toxic metabolites (formaldehyde, glycine and glyoxylate) are produced.

We assayed growth of wild-type, Δ*ttmR,* and Δ*efgA* strains during the transition to methylotrophy by subculturing stationary-phase, succinate-grown cells into fresh medium containing methanol as the sole carbon source. Both mutant strains displayed lag times that were comparable to each other but significantly longer (by ~ 6 hr) than those observed in wild-type (Table 2, Figure 5A). However, the growth rates and final yields of all strains were indistinguishable (Table 2). Cell viability assays uniformly showed that there was no statistically significant decrease in viable cell counts (WT vs. Δ*ttmR* p-value=0.223, WT vs. Δ*efgA* p-value=0.215) during the apparent lag phases and indicated that mutant strains take longer to enter exponential growth, rather than experiencing death (Figure 5C). The ability of strains to transition between distinct modes of metabolism was further probed in an analogous experiment, where methanol-grown cells (Figure

444 5A) were subcultured into fresh medium containing succinate as the sole carbon source; no growth
445 defect was observed (Figure 5B).

446 To further characterize the defect in the transition to methylotrophy of the Δ*ttmR* and Δ*efgA* strains,
447 we monitored formaldehyde accumulation in the culture supernatants. In wild-type, formaldehyde
448 accumulated in the supernatant and peaked at ~ 100 μM upon entry into exponential growth,
449 comparable to previously described results in *M. extorquens* AM1 (35). In the supernatants of the
450 Δ*ttmR* and Δ*efgA* mutants, formaldehyde accumulated to nearly 3-4X the levels observed in wild-
451 type (~ 275 and ~ 400 μM, respectively) demonstrating that formaldehyde resistant mutants have
452 perturbed formaldehyde metabolism (Figure 5D).

453 Collectively, these data show that during the transition to methylotrophy, formaldehyde imbalance
454 is exacerbated in the absence of TtmR or EfgA and suggest that both proteins are required for
455 formaldehyde homeostasis. Therefore, in mutant strains, there is a clear tradeoff between acquiring
456 formaldehyde resistance and the ability to adapt to methylotrophic growth.

457 **Phenotypic heterogeneity during the transition to methylotrophy.**

458 It has been previously observed that bacterial stressors can provoke phenotypic heterogeneity and,
459 recently, phenotypic heterogeneity in formaldehyde tolerance was demonstrated in wild-type
460 populations of unstressed *M. extorquens* PA1 (42). Here, in the presence of elevated formaldehyde,
461 individual cells experience a binary outcome and either tolerate formaldehyde from the onset of
462 exposure and grow or succumb to formaldehyde stress and die. As the transition to methylotrophy
463 leads to formaldehyde imbalance, we wanted to determine if the extended lag times of the Δ*ttmR*
464 and Δ*efgA* mutants during this transition were due to increased variance of individuals entering

465 exponential growth (i.e., some cells initiating growth after a longer time or not at all) or was
466 indicative of a change in the mean behavior of individuals without increased variance.

467 Tracking the entry into growth in populations by dilution of a membrane-intercalating dye in
468 individual cells revealed heterogeneous initiation of growth in Δ*ttmR* and Δ*efgA* strains. When
469 cells were transferred from one methanol-grown culture to fresh medium with methanol, all strains
470 displayed a gradual and uniform lessening in the distributions of per-cell fluorescence, indicating
471 uniform growth of cells within these populations (Figures 6 and S4). In contrast, following the
472 transition to methylotrophic growth, a notable skew, or split, in the distribution was observable by
473 9 hours. Most pronounced in the Δ*efgA* mutant, this result suggests the existence of a
474 subpopulation of nongrowing cells in the Δ*efgA* lineages, which is not effectively transitioning to
475 growth on methanol. The Δ*ttmR* lineages experience a similar delay; however, in this genotype,
476 the effect is seen as a rightward skew of the distribution rather than as two distinct peaks,
477 suggesting that not all cells survive the transition. This effect was dramatically diminished in the
478 wild-type strain, suggesting that it experiences more uniformity and less growth inhibition during
479 the transition between growth on different carbon substrates across members of the population.
480 This result is also consistent with bulk growth trends observed in the methylotrophic switch
481 (Figure 5).

482

DISCUSSION

During methylotrophic growth, all carbon flows through formaldehyde, a cytotoxic compound that can potentially damage myriad biomolecules. Accordingly, methylotrophs are more resistant to formaldehyde than non-methylotrophs (42). In large part, formaldehyde resistance can be attributed to the constitutively high expression and activity of Fae, which catalyzes the first step of formaldehyde oxidation and eliminates free formaldehyde from the cytoplasm. Despite this, formaldehyde pools in *M. extorquens* are elevated in comparison to non-methylotrophs (1, 46–49) and the mechanisms by which these greater pool sizes are tolerated and regulated are largely unknown, as are specific mechanisms of averting formaldehyde-induced cellular damage. Recent work uncovered the role of EfgA in directly sensing formaldehyde and acting to inhibit translation (7). The current work indicates that TtmR, a MarR-like transcription factor, is a second regulator in the formaldehyde stress response predicted to act at the level of transcription. TtmR regulates transcription of *efgA*, but the growth phenotypes of double mutants also indicate that TtmR regulates other targets beyond this. TtmR and EfgA each contribute to formaldehyde homeostasis and are particularly critical during the transition to methylotrophic metabolism. The combination of these distinct systems suggests that formaldehyde metabolism is monitored and managed across transcriptional and translational regulatory processes.

Without TtmR, *M. extorquens* does not display any obvious growth defects during methylotrophic growth, but instead, displays increased formaldehyde resistance. Increased formaldehyde resistance, as measured by growth in the presence of increasing formaldehyde concentrations, can be achieved by alleviating formaldehyde damage or by relaxing regulatory mechanisms that would otherwise prevent growth in potentially harmful conditions. Characterized formaldehyde stress response systems in bacteria prevent formaldehyde damage by formaldehyde detoxification and

506 are analogous to formaldehyde oxidation systems used by a variety of methylotrophs for C_1
507 utilization (21). In many organisms where formaldehyde stress has been investigated,
508 formaldehyde-induced DNA damage is often identified and cell damage and death are attributed
509 to genotoxicity (39, 40, 50). More recently however, formaldehyde-induced proteotoxicity has
510 been implicated in cytotoxicity in some human tissues (41), in synthetic methylotrophs (51), and
511 has been suggested by our own work in *M. extorquens* (7, 42). Therefore, other mechanisms of
512 formaldehyde resistance might activate appropriate DNA repair systems and/or heat shock proteins
513 to mitigate DNA and/or protein damage.

514 Surprisingly, in the transcriptome of the Δ*ttmR* mutant there are no DEGs that are obviously linked
515 to methylotrophic pathways, independent formaldehyde detoxifying enzymatic activities, or DNA
516 repair. Further, of the four genes grouped into Chaperone/Heat shock, three of them are
517 downregulated in the absence of TtmR. Functional groupings showed that the majority of DEGs
518 encode regulators, signaling proteins, stress response proteins, hypothetical proteins, and
519 transporters whose functions and physiological roles are unknown. This variety of DEGs suggests
520 that formaldehyde resistance may be the result of cumulative, coordinated responses from many
521 uncharacterized mechanisms.

522 Although increased formaldehyde resistance that emerges in strains lacking TtmR or EfgA could
523 be an advantageous trait in a methylotroph, we have demonstrated that a physiological and
524 ecological benefit of TtmR and EfgA is to speed the transition to methylotrophy when endogenous
525 formaldehyde is known to accumulate. Many *Methylobacterium/Methylorubrum* are plant-
526 associated and can use methanol derived from plants by pectin metabolism, among other
527 compounds (26, 52–56). Some, such as *M. extorquens* PA1, which was isolated from *Arabidopsis*
528 *thaliana*, are epiphytes and live on plant leaf surfaces (26). On leaf surfaces, methanol is released

529 from stomata, small pores in plant tissues that allow gas exchange (57). Methanol availability,
530 therefore, fluctuates as stomata open and close and is most abundant in the morning, upon the first
531 stomatal opening of the day (58, 59). To take advantage of this nutritional niche, *M. extorquens*
532 must quickly transition to methylotrophic metabolism, which necessarily includes production of a
533 metabolic stressor, formaldehyde (1, 45). Therefore, during this transition the physiological state
534 of *M. extorquens* must also be prepared for formaldehyde stress to occur. Here, TtmR and EfgA
535 were shown to be required for the optimal transition to methylotrophic growth and further, in their
536 absence, excess formaldehyde accumulation was observed, demonstrating dysregulation of
537 formaldehyde metabolism. On the phylloplane, the organism's native environment, where
538 methanol emissions are transient and come in bursts, loss of TtmR or EfgA would likely be
539 disadvantageous and render *M. extorquens* less competitive within its ecological niche where
540 methanol capture is important.

541 The transition to methylotrophy in *M. extorquens* AM1 has been previously investigated with
542 systems biology and genetic approaches, but did not identify either the *ttmR* or *efgA* locus (1, 5, 6,
543 45). There, investigators found that upon transitioning from the multi-carbon growth substrate
544 succinate to the single-carbon growth substrate methanol, cells have a lag in carbon assimilation
545 and experience a transient imbalance in formaldehyde metabolism, with formaldehyde
546 accumulating such that it was secreted into the growth medium (45). Further investigation revealed
547 that in adapting cells, carbon flux restriction was mediated by methenyl-dH$_4$MPT, an intermediate
548 in the formaldehyde dissimilation that directly inhibits MtdA, the enzyme that generates the
549 substrate for entry into the Serine Cycle assimilation pathway and may regulate Fae activity by an
550 unknown mechanism (1). These authors propose carbon flux restriction is an adaptive strategy that
551 minimizes the accumulation of toxic metabolites generated in methylotrophic pathways, including

552 formaldehyde. As strains defective in dH_4MPT biosynthesis (Δ*mptG)* were previously shown to
553 be more methanol (i.e., formaldehyde) sensitive in the absence of EfgA (7), we conclude that
554 EfgA-mediated formaldehyde homeostasis does not involve methenyl-dH_4MPT.

555 All of the phenotypes of the Δ*ttmR* mutant were mirrored in the Δ*efgA* mutant; therefore, we
556 considered the possibility that TtmR and EfgA were interconnected. Specifically, we considered
557 whether TtmR was a positive regulator of *efgA* expression. The transcriptomic data initially
558 seemed to support this possibility, as *efgA* expression was two-fold lower in the Δ*ttmR* mutant.
559 However, genetic analysis showed that TtmR and EfgA elimination could cause formaldehyde
560 resistance and a defective switch to methylotrophy independent of one another. Thus, this work
561 has identified TtmR as a second formaldehyde stress response protein, which can act
562 independently of EfgA and a role for TtmR and EfgA in formaldehyde tolerance and homeostasis.
563 Given the phenotypic overlap of these proteins, it is still possible, and perhaps quite likely, that
564 they independently impact a common cellular function that results in the formaldehyde-associated
565 phenotypes observed. Alternatively, the overlap may represent that *efgA* expression is just one of
566 multiple mechanisms that TtmR exerts its effects on formaldehyde homeostasis.

567 Herein, we demonstrate that achieving formaldehyde resistance through the loss of TtmR or EfgA
568 comes at a cost, as increased formaldehyde resistance simultaneously limits the adaptability of *M.*
569 *extorquens* to methylotrophic metabolism. The formaldehyde accumulation observed during the
570 transition to methylotrophy suggest that strains lacking TtmR and EfgA achieve formaldehyde
571 resistance by losing their ability to sense and respond to perturbations in formaldehyde
572 homeostasis, rather than by simply improving cellular processes that reduce formaldehyde
573 damage. Interestingly, this tradeoff can be avoided, as mutations that permitted growth on
574 formaldehyde that occurred in other loci, *def* and *efgB*, did not cause a defect in the transition to

575 methylotrophy (Figure S5). Therefore, the transcriptomic profile observed in strains lacking TtmR
576 likely reflects relaxing a combination of cellular components that typically govern formaldehyde
577 balance as well as those that are responding to the resulting formaldehyde perturbation. The variety
578 of DEGs, which includes many regulators, suggest that TtmR is part of a larger gene regulatory
579 network. Additionally, it appears that both TtmR and EfgA are required for *M. extorquens* to
580 rapidly shift from growth on multi-carbon substrates to growth on one-carbon substrates and may
581 be of general importance for facultative methylotrophs.

582

583 **Figure 1. Formaldehyde-evolved isolates have increased formaldehyde resistance.**

584 Wild-type (CM2730, black circles) and mutant strains harboring loss-of-function mutations in
585 Δ*efgA* (CM3745, blue triangles) or $ttmR^{EVO}$ (CM3919, purple squares) were grown in liquid MP
586 medium with 0, 2, 4, 6, 8, or 10 mM exogenous formaldehyde. Final yields are shown when
587 formaldehyde was provided as a sole source of carbon and energy (A) or as a stressor when
588 methanol (B), or succinate (C) was provided as the primary carbon source. *Error bars* represent
589 the standard error of the mean of biological replicates.

590 **Figure 2. Deletion of *ttmR* recapitulates increased formaldehyde resistance.**

591 Wild-type (CM2730, circles) and the constructed Δ*ttmR* mutant (CM4732, squares) were grown
592 in liquid MP medium containing 0, 4, or 6 mM exogenous formaldehyde (indicated by black,
593 yellow, or red symbols, respectively). Absorbance up to 48 hours was measured to assess growth
594 when formaldehyde was provided as a sole source of carbon and energy (A) or as a stressor when
595 methanol (B), or succinate (C) was provided as the primary carbon source. *Error bars* represent
596 the standard error of the mean of biological replicates.

597 **Figure 3. Differentially expressed genes in the Δ*ttmR* mutant.**

598 RNA-sequencing analysis was performed on wild-type and the Δ*ttmR* mutant with cells in the
599 early exponential phase of growth on methanol. The $\log_2$ fold changes (Log_2FC) in gene expression
600 of the Δ*ttmR* mutant were calculated relative to wild-type. Adjusted p-values were also calculated.
601 Differentially expressed genes are defined as having a $Log_2FC > 1.0$ and $p_{adj} < 0.05$; each bar
602 represents an individual gene. Horizontal bars over clusters of genes indicate two or more adjacent
603 genes with the number of genes clustered indicated above the bar. Gene annotations are provided
604 in Table 1.

Figure 4. The Δ*ttmR* Δ*efgA* double mutant has increased formaldehyde resistance.

Growth of the Δ*ttmR* (CM4732, purple squares), Δ*efgA* mutant (CM3745, blue triangles), and Δ*ttmR* Δ*efgA* double mutant (CM4733, pink diamonds) was quantified in liquid MP medium (succinate) containing 6 mM formaldehyde. *Error bars* represent the standard error of mean of biological replicates.

Figure 5. The Δ*ttmR* and Δ*efgA* mutants are defective in the transition to methylotrophy.

The wild-type (CM2730, black circles), Δ*ttmR* mutant (CM4732, purple squares), and Δ*efgA* mutant (CM3745, blue triangles) were first acclimated to succinate in liquid MP medium. Their growth was then assayed upon their inoculation to methanol-based medium by absorbance (A) and cell viability (C). Formaldehyde concentrations in the growth medium was measured by a colorimetric assay (D). After reaching stationary phase, the methanol-grown cultures were subcultured to succinate-based medium and assayed for growth by absorbance (B). We used a >15% increase from starting absorbance (dashed line) constituted a threshold that marked the end of lag phase. *Error bars* represent the standard error of mean of biological replicates. In panel D, individual values are shown and the mean is indicated.

Figure 6. Distribution of cell division during growth on methanol varies depending on the starting growth substrate.

Following acclimation to growth on either single- (methanol) or multi-carbon (succinate) sources, stationary phase cells were labelled with a fluorescent dye that intercalates into the cell membrane and thereby allows tracking of cell division through dilution of the starting signal. Patterns of cell division were measured following 24 hours of growth in methanol (A) or during shifts from succinate to methanol (B) by measuring fluorescence of individual cells within the populations using flow cytometry. The resulting data is displayed as distributions of fluorescence

628 intensity that demonstrate how a population does or does not migrate (grow and divide) over
629 time. Data is plotted as histograms of per-cell fluorescence intensity (measured at the emission
630 wavelength of 525 nm, FITC channel) of cell populations at different time points across growth.
631 Each line in a panel represents cell events surveyed for a single (of three) biological replicate
632 within an equivalent number of cells.
633

Table 1. Genes differentially expressed in a Δ*ttmR* mutant.

RNA-sequencing analysis was performed on wild-type and the Δ *ttmR* mutant with cells in the early exponential phase of growth on methanol. The $\log_2$ fold changes (Log_2FC) in gene expression of the Δ *ttmR* mutant were calculated relative to wild-type. Adjusted p-values were also calculated. Genes detailed here have a $Log_2FC > 1.0$ and $p_{adj} < 0.05$.

Table 2. Growth during carbon substrate transitions.

Growth of succinate- or methanol-grown stationary phase cells subcultured into fresh medium with 15 mM methanol or 3.5 mM succinate, respectively, was monitored. Error shown represents standard error of the mean of biological replicates. Error was not provided for lag time as resolution at low cell densities is not sensitive enough to quantify. A two-tailed Student's t-test was performed to identify statistically significant differences in final yields or growth rates between growth rates (p-value < 0.05).

Figure S1. Treatment of a Δ*ttmR* mutant with alternative aldehydes.

Growth of wild-type (CM2730, black circles) and the *ttmR*^{EVO} mutant (CM3919, purple squares) was quantified in liquid MP medium (succinate) with the addition of (A) 2 mM formaldehyde, (B) 1.25 mM acetaldehyde, (C) 2.5 mM butyraldehyde, (D) 2.5 mM propionaldehyde, (E) 1.25 mM glyoxal, and (F) 0.157 mM glutaraldehyde. Growth of wild-type was quantified in the same medium (succinate) without aldehydes and is superimposed in all panels for reference (CM2730, gray circles). Growth of CM3919 was indistinguishable from wild-type in the absence of aldehyde stress; data were excluded for visual simplicity. *Error bars* represent the standard error of mean of biological replicates.

Figure S2. Histogram of adjusted p-values and Log_2FC values for RNA-Seq.

The distributions of calculated (A) p-values and (B) Log_2FC values are shown. Bins are defined in increments of 0.05. The red line shows the curve fit to the Gaussian distribution of Log_2FC values.

Figure S3. Distribution of DEGs in different cellular processes.

The pie graph shows the distribution of differentially expressed genes in functional categories according to cellular process. Categories were assigned by annotation and inference from the presence of specific Pfam domains. When function could not be inferred (lack of Pfam domain, domain of unknown function), genes were classified as Hypothetical (orange) and when function was only represented once, genes were classified as Singletons (white). Number of genes in each category is indicated as well as the proportion are up- or down-regulated (arrows).

Figure S4. Heterogeneity during the transition to methylotrophic metabolism.

668 Following acclimation to growth on either single- or multi-carbon sources, stationary phase cells
669 were labelled with a fluorescent dye that intercalates into the cell membrane and thereby allows
670 tracking of cell division through dilution of the starting signal. Patterns of growth were tracked in
671 continued growth in methanol (left column) or during shifts from succinate to methanol (right
672 column) by measuring fluorescence of individual cells within the populations using flow
673 cytometry at time points over the course of population growth. The resulting data is displayed as
674 distributions of fluorescence intensity that demonstrate how a population does or does not migrate
675 (grow) over time. During continued growth on methanol, there is a uniform decrease in the
676 fluorescence distribution for the whole population for each of the three strains (left column). In
677 contrast, a distinct shoulder or even a second peak of the distribution representing cells that
678 maintain high fluorescence indicates that not all cells have initiated growth simultaneously, if at
679 all. This second mode of the distribution is seen, at least transiently, for all genotypes but is most
680 pronounced in magnitude and time that it remains a part of the population for the Δ*efgA* strain.
681 Data is plotted as histograms of per-cell fluorescence intensity (measured at the emission
682 wavelength of 525 nm, FITC channel) of cell populations at different time points across growth.
683 Each timepoint in a panel represents cell events surveyed within an equivalent volume of growing
684 culture volume. Each panel depicts a single representativebiological replicate.

685

686 **Figure S5. Evolved strains with mutations in other loci leading to enhanced formaldehyde**
687 **growth are not defective in transition to methylotrophy.**

688 Strains with single-base pair mutations in *def* (CM3908, brown diamonds) and *efgB* (CM3783,
689 green inverted triangles and CM3837, lime-green triangles) were screened for their influence on
690 lag times during carbon source switch that required the cells to transition to methylotrophic growth.

691 The wild-type (CM2730, black, no symbols), Δ*ttmR* mutant (CM4732, purple squares), and Δ*efgA*
692 mutant (CM3745, blue triangles) were included as controls and/or reference points. Succinate-
693 acclimated strains were subcultured into fresh liquid MP medium with methanol as the carbon
694 source and growth was assayed by absorbance. We used a >15% increase from starting absorbance
695 (dashed line) constituted a threshold that marked the end of lag phase. *Error bars* represent the
696 standard error of mean of biological replicates.

697

Table S1. Bacterial strains[a] and plasmids[b].

Table S2. Growth of the Δ*ttmR* mutant is comparable to wild-type in the absence of formaldehyde stress.

M. extorquens was grown in MPIPES medium with 3.5 mM succinate or 15 mM methanol as the sole source of carbon and energy. Error shown represents standard from mean of biological replicates. Error was not provided for lag time due to poor resolution at low cell densities. A two-tailed Student's t-test was performed to identify statistically significant differences in final yields or growth rates between growth rates (p-value < 0.05).

Table S3. The Δ*ttmR* mutant does not mediate a general stress response.

The wild-type and the $ttmR^{EVO}$ mutant were subjected to various stressors, including a panel of antibiotics, hydrogen peroxide, ethanol, and heat. The resulting stress was phenotypically manifested by growth inhibition as indicated by zones of inhibition (cm), changes in viability (CFU/mL), or qualitative decrease in colony size.

Table S4. Transcriptomic analysis of the methylotrophy genes.

715 REFERENCES

716 6. Martinez-Gomez NC, Good NM, Lidstrom ME. 2015. Methenyl-
717 Dephosphotetrahydromethanopterin Is a Regulatory Signal for Acclimation to Changes in
718 Substrate Availability in *Methylobacterium extorquens* AM1. J Bacteriol 197:2020–2026.

719 2. Vorholt JA, Marx CJ, Lidstrom ME, Thauer RK. 2000. Novel Formaldehyde-Activating Enzyme
720 in *Methylobacterium extorquens* AM1 Required for Growth on Methanol. J Bacteriol 182:6645–
721 6650.

722 3. Chistoserdova L, Vorholt JA, Thauer RK, Lidstrom ME. 1998. C1 transfer enzymes and
723 coenzymes linking methylotrophic bacteria and methanogenic Archaea. Science 281:99–102.

724 4. Marx CJ, Chistoserdova L, Lidstrom ME. 2003. Formaldehyde-detoxifying role of the
725 tetrahydromethanopterin-linked pathway in *Methylobacterium extorquens* AM1. J Bacteriol
726 185:7160–7168.

727 5. Marx CJ, Van Dien SJ, Lidstrom ME. 2005. Flux analysis uncovers key role of functional
728 redundancy in formaldehyde metabolism. PLoS Biol 3:e16.

729 6. Crowther GJ, Kosály G, Lidstrom ME. 2008. Formate as the main branch point for
730 methylotrophic metabolism in *Methylobacterium extorquens* AM1. J Bacteriol 190:5057–5062.

731 7. Bazurto JV, Nayak DD, Ticak T, Davlieva M, Lambert LB, Quates, CJ, Patel JS, Ytreberg FM,
732 Shamoo Y, Marx CJ. 2020. EfgA halts bacterial translation in response to intracellular
733 formaldehyde. BioRxiv [Preprint]. 2020 bioRxiv 343392 [submitted 2020 Oct 16].

734

738. Piatkov KI, Vu TTM, Hwang C-S, Varshavsky A. 2015. Formyl-methionine as a degradation
736 signal at the N-termini of bacterial proteins. Microb Cell Fact 2:376–393.

739. George AM, Levy SB. 1983. Gene in the major cotransduction gap of the *Escherichia coli* K-12
738 linkage map required for the expression of chromosomal resistance to tetracycline and other
739 antibiotics. J Bacteriol 155:541–548.

7400. George AM, Levy SB. 1983. Amplifiable resistance to tetracycline, chloramphenicol, and other
741 antibiotics in *Escherichia coli*: involvement of a non-plasmid-determined efflux of tetracycline. J
742 Bacteriol 155:531–540.

7431. Cohen SP, Yan W, Levy SB. 1993. A multidrug resistance regulatory chromosomal locus is
744 widespread among enteric bacteria. J Infect Dis 168:484–488.

7452. Cohen SP, Hächler H, Levy SB. 1993. Genetic and functional analysis of the multiple antibiotic
746 resistance (*mar*) locus in *Escherichia coli*. J Bacteriol 175:1484–1492.

7473. Martin RG, Nyantakyi PS, Rosner JL. 1995. Regulation of the multiple antibiotic resistance
748 (*mar*) regulon by marORA sequences in *Escherichia coli*. J Bacteriol 177:4176–4178.

7494. Martin RG, Rosner JL. 1995. Binding of purified multiple antibiotic-resistance repressor protein
750 (MarR) to *mar* operator sequences. Proc Natl Acad Sci U S A 92:5456–5460.

7515. Chubiz LM, Rao CV. 2010. Aromatic acid metabolites of *Escherichia coli* K-12 can induce the
752 *marRAB* operon. J Bacteriol 192:4786–4789.

7536. Seoane AS, Levy SB. 1995. Identification of new genes regulated by the *marRAB* operon in
754 *Escherichia coli*. J Bacteriol 177:530–535.

755 17. Seoane AS, Levy SB. 1995. Characterization of MarR, the repressor of the multiple antibiotic
756 resistance (*mar*) operon in *Escherichia coli*. J Bacteriol 177:3414–3419.

757 18. Sharma P, Haycocks JRJ, Middlemiss AD, Kettles RA, Sellars LE, Ricci V, Piddock LJV,
758 Grainger DC. 2017. The multiple antibiotic resistance operon of enteric bacteria controls DNA
759 repair and outer membrane integrity. Nat Commun 8:1444.

760 19. Grove A. 2017. Regulation of Metabolic Pathways by MarR Family Transcription Factors.
761 Comput Struct Biotechnol J 15:366–371.

762 20. Yurimoto H, Hirai R, Matsuno N, Yasueda H, Kato N, Sakai Y. 2005. HxlR, a member of the
763 DUF24 protein family, is a DNA-binding protein that acts as a positive regulator of the
764 formaldehyde-inducible *hxlAB* operon in *Bacillus subtilis*. Mol Microbiol 57:511–519.

765 21. Chen NH, Djoko KY, Veyrier FJ, McEwan AG. 2016. Formaldehyde Stress Responses in
766 Bacterial Pathogens. Front Microbiol 7:257.

767 22. Yasueda H, Kawahara Y, Sugimoto S. 1999. *Bacillus subtilis yckG* and *yckF* encode two key
768 enzymes of the ribulose monophosphate pathway used by methylotrophs, and *yckH* is required
769 for their expression. J Bacteriol 181:7154–7160.

770 23. Parke D, Ornston LN. 2003. Hydroxycinnamate (*hca*) catabolic genes from Acinetobacter sp.
771 strain ADP1 are repressed by HcaR and are induced by hydroxycinnamoyl-coenzyme A
772 thioesters. Appl Environ Microbiol 69:5398–5409.

773 24. Tropel D, van der Meer JR. 2004. Bacterial transcriptional regulators for degradation pathways
774 of aromatic compounds. Microbiol Mol Biol Rev 68:474–500, table of contents.

775 25. Davis JR, Brown BL, Page R, Sello JK. 2013. Study of PcaV from *Streptomyces coelicolor*
776 yields new insights into ligand-responsive MarR family transcription factors. Nucleic Acids Res
777 41:3888–3900.

778 26. Knief C, Frances L, Vorholt JA. 2010. Competitiveness of diverse *Methylobacterium* strains in
779 the phyllosphere of *Arabidopsis thaliana* and identification of representative models, including
780 M. extorquens PA1. Microb Ecol 60:440–452.

781 27. Marx CJ, Bringel F, Chistoserdova L, Moulin L, Farhan Ul Haque M, Fleischman DE, Gruffaz
782 C, Jourand P, Knief C, Lee M-C, Muller EEL, Nadalig T, Peyraud R, Roselli S, Russ L,
783 Goodwin LA, Ivanova N, Kyrpides N, Lajus A, Land ML, Médigue C, Mikhailova N, Nolan M,
784 Woyke T, Stolyar S, Vorholt JA, Vuilleumier S. 2012. Complete genome sequences of six
785 strains of the genus *Methylobacterium*. J Bacteriol 194:4746–4748.

786 28. Green PN, Ardley JK. 2018. Review of the genus *Methylobacterium* and closely related
787 organisms: a proposal that some *Methylobacterium* species be reclassified into a new genus,
788 Methylorubrum gen. nov. Int J Syst Evol Microbiol 68:2727–2748.

789 29. Delaney NF, Kaczmarek ME, Ward LM, Swanson PK, Lee M-C, Marx CJ. 2013. Development
790 of an optimized medium, strain and high-throughput culturing methods for *Methylobacterium*
791 *extorquens*. PLoS One 8:e62957.

792 30. Marx CJ. 2008. Development of a broad-host-range *sacB*-based vector for unmarked allelic
793 exchange. BMC Res Notes 1:1.

794 31. Nash T. 1953. The colorimetric estimation of formaldehyde by means of the Hantzsch reaction.
795 Biochem J 55:416–421.

792 32. FastQC: A quality control tool for high throughput sequence data. Babraham Bioinformatics.

793 33. Bolger AM, Lohse M, Usadel B. 2014. Trimmomatic: a flexible trimmer for Illumina sequence
794 data. Bioinformatics 30:2114–2120.

795 34. Kim D, Langmead B, Salzberg SL. 2015. HISAT: a fast spliced aligner with low memory
796 requirements. Nat Methods 12:357–360.

797 35. Trapnell C, Roberts A, Goff L, Pertea G, Kim D, Kelley DR, Pimentel H, Salzberg SL, Rinn JL,
798 Pachter L. 2012. Differential gene and transcript expression analysis of RNA-seq experiments
799 with TopHat and Cufflinks. Nat Protoc 7:562–578.

800 36. Liao Y, Smyth GK, Shi W. 2019. The R package Rsubread is easier, faster, cheaper and better
801 for alignment and quantification of RNA sequencing reads. Nucleic Acids Res 47:e47.

802 37. Love MI, Huber W, Anders S. 2014. Moderated estimation of fold change and dispersion for
803 RNA-seq data with DESeq2. Genome Biol 15:550.

804 38. Gourion B, Francez-Charlot A, Vorholt JA. 2008. PhyR is involved in the general stress response
805 of *Methylobacterium extorquens* AM1. J Bacteriol 190:1027–1035.

806 39. Kawanishi M, Matsuda T, Yagi T. 2014. Genotoxicity of formaldehyde: molecular basis of DNA
807 damage and mutation. Front Environ Sci Eng China 2:36.

808 40. Grafstrom RC, Fornace AJ Jr, Autrup H, Lechner JF, Harris CC. 1983. Formaldehyde damage to
809 DNA and inhibition of DNA repair in human bronchial cells. Science 220:216–218.

41. Ortega-Atienza S, Rubis B, McCarthy C, Zhitkovich A. 2016. Formaldehyde Is a Potent Proteotoxic Stressor Causing Rapid Heat Shock Transcription Factor 1 Activation and Lys48-Linked Polyubiquitination of Proteins. Am J Pathol 186:2857–2868.

42. Lee JA, Riazi S, Nemati S, Bazurto JV, Vasdekis AE, Ridenhour BJ, Remien CH, Marx CJ. 2019. Microbial phenotypic heterogeneity in response to a metabolic toxin: Continuous, dynamically shifting distribution of formaldehyde tolerance in *Methylobacterium extorquens* populations. PLoS Genet 15:e1008458.

43. Nunn DN, Lidstrom ME. 1986. Isolation and complementation analysis of 10 methanol oxidation mutant classes and identification of the methanol dehydrogenase structural gene of *Methylobacterium* sp. strain AM1. J Bacteriol 166:581–590.

44. Anderson DJ, Lidstrom ME. 1988. The *moxFG* region encodes four polypeptides in the methanol-oxidizing bacterium *Methylobacterium* sp. strain AM1. J Bacteriol 170:2254–2262.

45. Skovran E, Crowther GJ, Guo X, Yang S, Lidstrom ME. 2010. A systems biology approach uncovers cellular strategies used by *Methylobacterium extorquens* AM1 during the switch from multi- to single-carbon growth. PLoS One 5:e14091.

46. Müller JEN, Meyer F, Litsanov B, Kiefer P, Potthoff E, Heux S, Quax WJ, Wendisch VF, Brautaset T, Portais J-C, Vorholt JA. 2015. Engineering *Escherichia coli* for methanol conversion. Metab Eng 28:190–201.

47. Heck HD, Casanova-Schmitz M, Dodd PB, Schachter EN, Witek TJ, Tosun T. 1985. Formaldehyde (CH2O) concentrations in the blood of humans and Fischer-344 rats exposed to CH2O under controlled conditions. Am Ind Hyg Assoc J 46:1–3.

48. Luo W, Li H, Zhang Y, Ang CY. 2001. Determination of formaldehyde in blood plasma by high-performance liquid chromatography with fluorescence detection. J Chromatogr B Biomed Sci Appl 753:253–257.

49. Nagy K, Pollreisz F, Takáts Z, Vékey K. 2004. Atmospheric pressure chemical ionization mass spectrometry of aldehydes in biological matrices. Rapid Commun Mass Spectrom 18:2473–2478.

50. Takahashi K, Morita T, Kawazoe Y. 1985. Mutagenic characteristics of formaldehyde on bacterial systems. Mutat Res 156:153–161.

51. Chen FY-H, Jung H-W, Tsuei C-Y, Liao JC. 2020. Converting *Escherichia coli* to a Synthetic Methylotroph Growing Solely on Methanol. Cell 182:933–946.e14.

52. Anthony C. 1982. The biochemistry of methylotrophs. Academic press London.

53. Corpe WA, Rheem S. 1989. Ecology of the methylotrophic bacteria on living leaf surfaces. FEMS Microbiol Ecol.

54. Van Dien SJ, Okubo Y, Hough MT, Korotkova N, Taitano T, Lidstrom ME. 2003. Reconstruction of C(3) and C(4) metabolism in *Methylobacterium extorquens* AM1 using transposon mutagenesis. Microbiology 149:601–609.

55. Sy A, Timmers ACJ, Knief C, Vorholt JA. 2005. Methylotrophic metabolism is advantageous for *Methylobacterium extorquens* during colonization of *Medicago truncatula* under competitive conditions. Appl Environ Microbiol 71:7245–7252.

854 56. Müller DB, Vogel C, Bai Y, Vorholt JA. 2016. The Plant Microbiota: Systems-Level Insights
855 and Perspectives. Annu Rev Genet 50:211–234.

856 57. Abanda-Nkpwatt D, Müsch M, Tschiersch J, Boettner M, Schwab W. 2006. Molecular
857 interaction between *Methylobacterium extorquens* and seedlings: growth promotion, methanol
858 consumption, and localization of the methanol emission site. J Exp Bot 57:4025–4032.

859 58. Nemecek-Marshall M, MacDonald RC, Franzen JJ, Wojciechowski CL, Fall R. 1995. Methanol
860 Emission from Leaves (Enzymatic Detection of Gas-Phase Methanol and Relation of Methanol
861 Fluxes to Stomatal Conductance and Leaf Development). Plant Physiol 108:1359–1368.

862 59. Hüve K, Christ MM, Kleist E, Uerlings R, Niinemets U, Walter A, Wildt J. 2007. Simultaneous
863 growth and emission measurements demonstrate an interactive control of methanol release by
864 leaf expansion and stomata. J Exp Bot 58:1783–1793.

865 60. Michener JK, Vuilleumier S, Bringel F, Marx CJ. 2016. Transfer of a Catabolic Pathway for
866 Chloromethane in *Methylobacterium* Strains Highlights Different Limitations for Growth with
867 Chloromethane or with Dichloromethane. Frontiers in Microbiology.

868

869

870

87 Figure 1

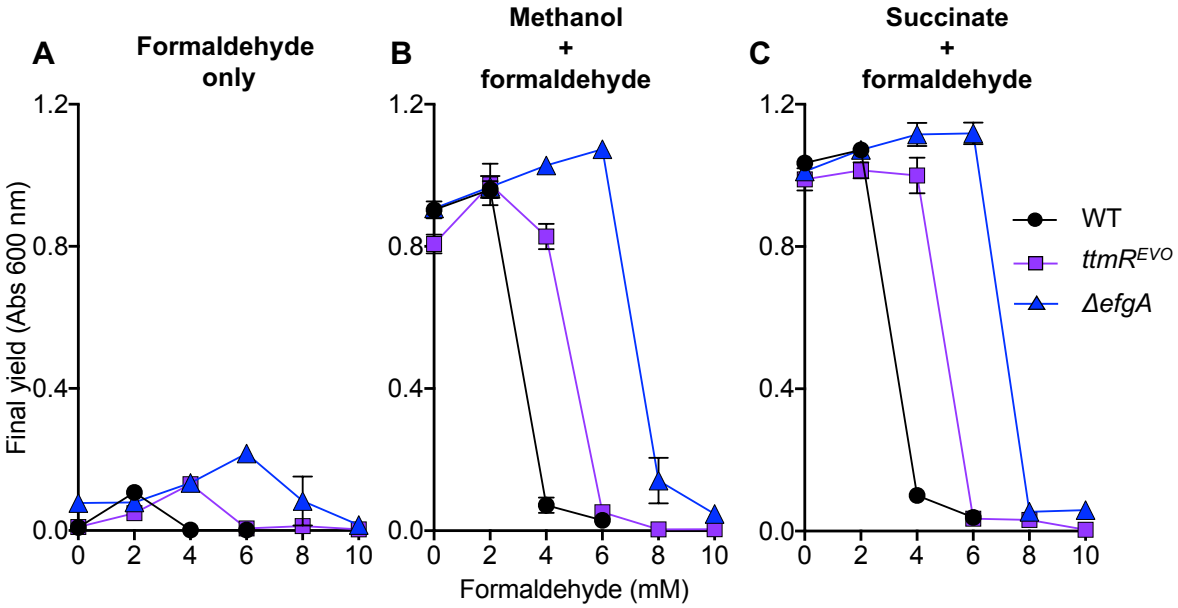

87

873

874 Figure 2

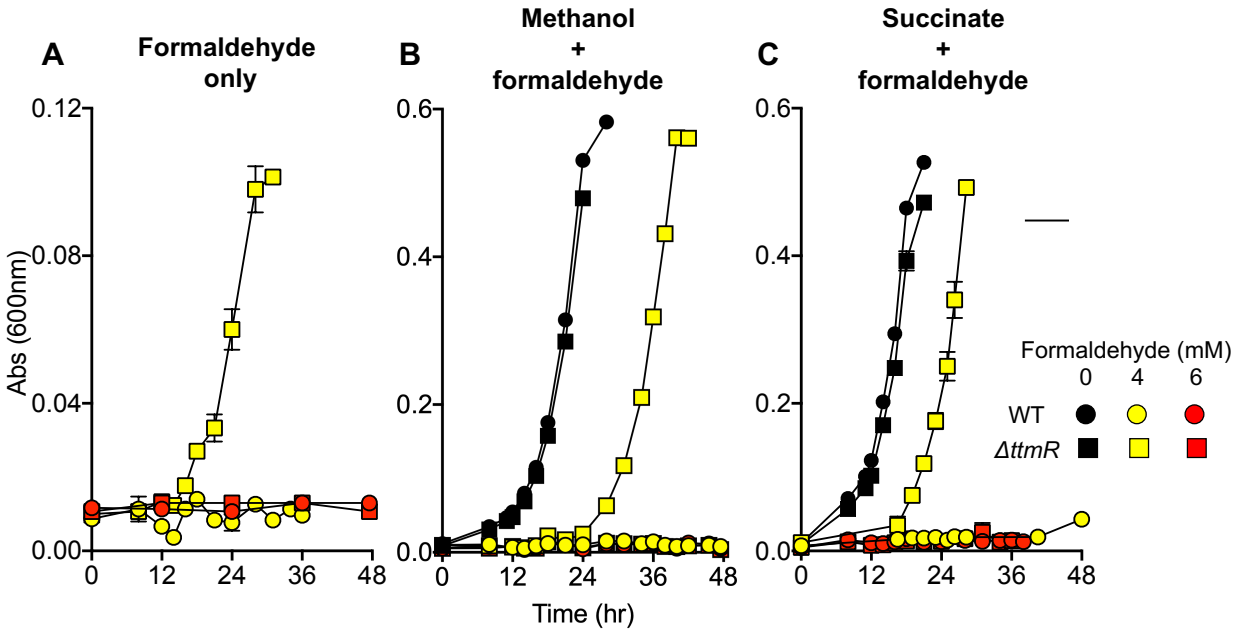

875

876

Figure 3

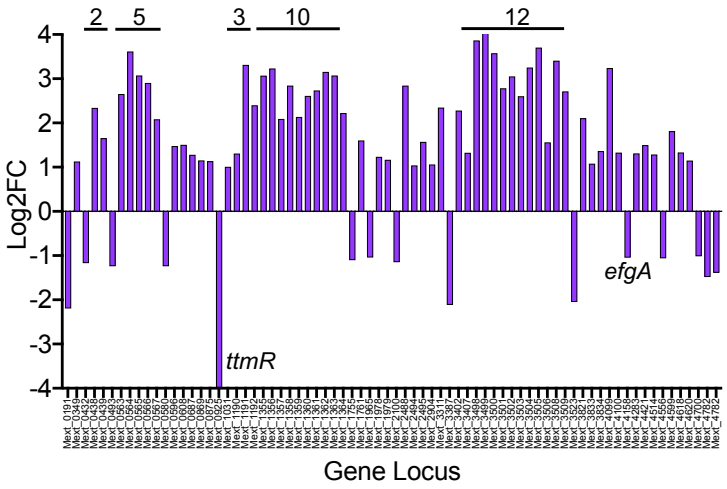

Figure 4

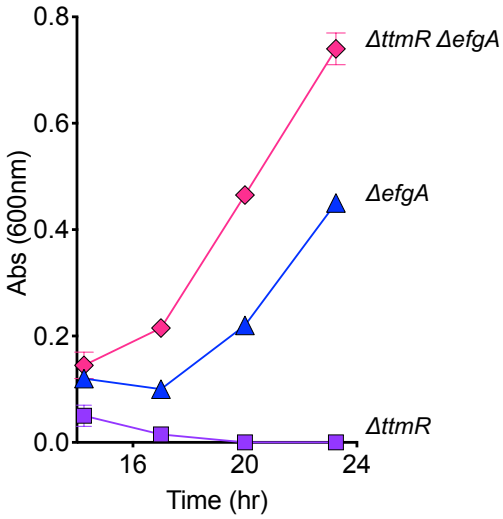

882 Figure 5

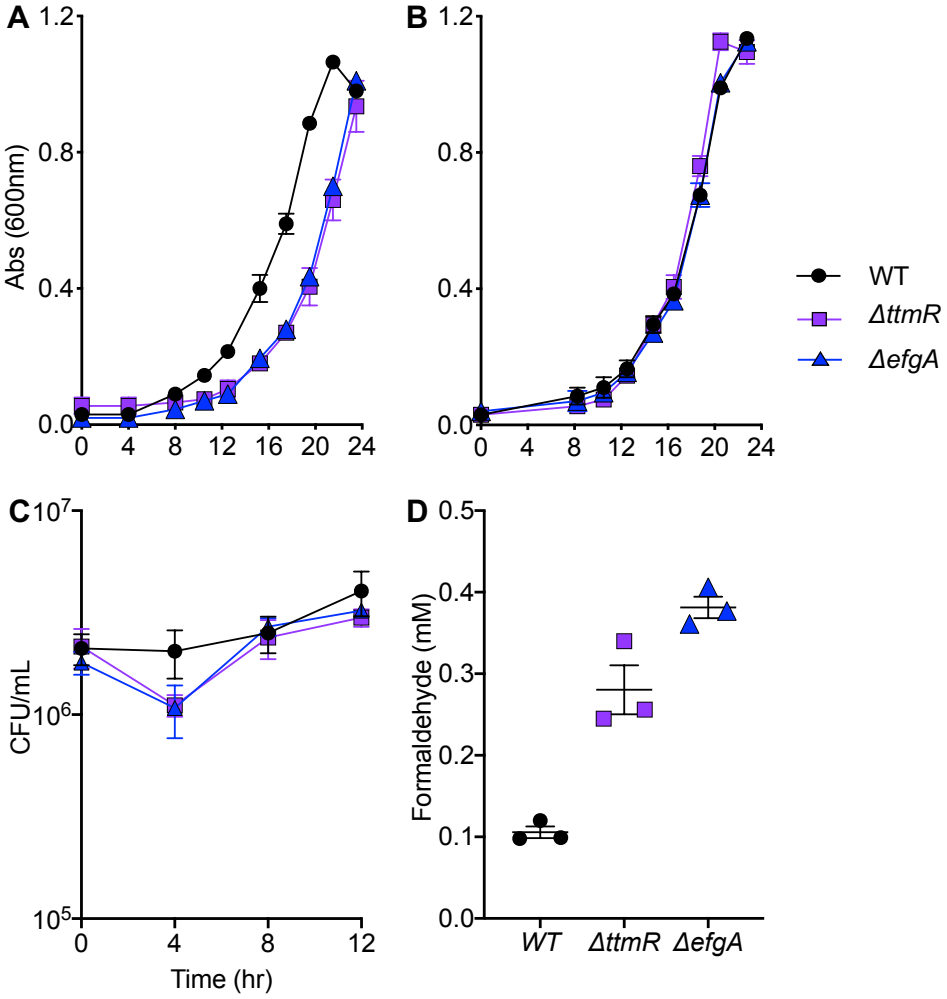

883

884

885Figure 6

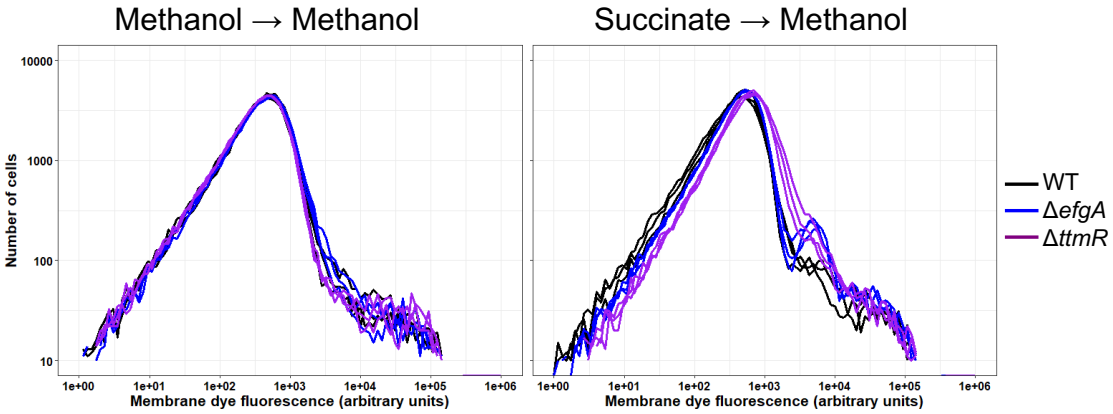

886

887

888 Table 1

889

Locus	Annotation (RefSeq)	Functional category	Log_2FC	p_{adj}
Mext_0044	hypothetical protein	Hypothetical	1.015	3.00E-3
Mext_0191	chemotaxis sensory transducer	Chemotaxis	-2.189	2.81E-129
Mext_0349	flagellin domain protein	Motility	1.121	8.86E-17
Mext_0432	ROSMUCR transcriptional regulator	Regulatory	-1.166	8.85E-44
Mext_0438	hypothetical protein	Signaling	2.335	1.36E-143
Mext_0439	hypothetical protein	Regulatory	1.652	1.24E-25
Mext_0493	hypothetical protein	Inclusion bodies	-1.235	2.44E-16
Mext_0563	acetate kinase	Central carbon metabolism	2.647	1.15E-124
Mext_0564	secretion protein HlyD family protein	Transport	3.610	0.00
Mext_0565	ABC transporter related	Transport	3.068	6.09E-291
Mext_0566	ABC-2 type transporter	Transport	2.898	1.08E-144
Mext_0567	Phosphoketolase	Central carbon metabolism	2.076	4.73E-148
Mext_0580	pseudogene	Pseudogene	-1.234	8.45E-38
Mext_0596	response regulator receiver	Regulatory	1.472	3.29E-81
Mext_0608	helix-turn-helix- domain containing protein AraC type	Regulatory	1.501	1.27E-44
Mext_0687	flagellar FlbT family protein	Motility	1.274	3.95E-35
Mext_0869	hypothetical protein	Stress (oxidative)	1.149	5.60E-10
Mext_0875	PAS sensor protein	Signaling (heat shock)	1.131	5.67E-37
Mext_0925	regulatory protein MarR	MarR	-9.624	1.38E-95
Mext_1031	glycerone kinase	Central carbon metabolism	1.002	6.93E-21
Mext_1190	PAS sensor protein	Signaling	1.304	1.92E-64
Mext_1191	membrane protein of uknown function UCP014873	Membrane DUF	3.307	0.00
Mext_1192	67 kDa myosin-cross-reactive antigen family protein	Stress (FA metabolism)	2.395	1.81E-143
Mext_1355	UspA domain protein	Stress	3.064	0.00
Mext_1356	cytochrome c class I	Cytochrome metabolism	3.227	0.00
Mext_1357	cyclic nucleotide-binding	Regulatory (cNMP)	2.086	6.65E-176
Mext_1358	ABC transporter related	Transport	2.837	2.01E-249
Mext_1359	ABC transporter related	Transport	2.131	9.30E-160
Mext_1360	cytochrome bd ubiquinol oxidase subunit I	Cytochrome metabolism	2.607	1.66E-216
Mext_1361	cytochrome d ubiquinol oxidase, subunit II	Cytochrome metabolism	2.728	2.92E-238
Mext_1362	*cyd* operon protein YbgT	Cytochrome metabolism	3.150	2.69E-256
Mext_1363	regulatory protein DeoR	Regulatory (sugar)	3.069	0.00
Mext_1364	amidase	Translation (tRNA charging)	2.218	7.97E-68

Mext_1755	aminoglycoside phosphotransferase	Signaling (phosphotransferase)	-1.098	7.26E-27
Mext_1761	methionine-*R*-sulfoxide reductase	Stress (oxidative), Regulatory (PTM)	1.598	2.08E-37
Mext_1965	response regulator receiver	Signaling	-1.037	8.82E-35
Mext_1978	diguanylate cyclase	Signaling (c-di-GMP)	1.230	1.73E-37
Mext_1979	hypothetical protein	hypothetical	1.160	1.62E-08
Mext_2100	hypothetical protein	Hypothetical (transport)	-1.145	4.33E-38
Mext_2114	hypothetical protein	Hypothetical	1.186	6.88E-3
Mext_2488	OsmC family protein	Stress (oxidative)	2.837	2.28E-184
Mext_2494	conserved hypothetical membrane spanning protein	Hypothetical (membrane)	1.035	2.75E-10
Mext_2495	CsbD family protein	Stress	1.568	2.67E-19
Mext_2904	hypothetical protein	Regulatory (stress)	1.055	2.33E-10
Mext_3311	hypothetical protein	Hypothetical	2.342	4.15E-117
Mext_3387	hypothetical protein	Hypothetical	-2.109	2.83E-46
Mext_3402	hypothetical protein	Hypothetical	2.275	2.38E-121
Mext_3407	ABC transporter related	Transport	1.319	3.12E-06
Mext_3498	heat shock protein Hsp20	Chaperone/Heat shock	3.861	0.00
Mext_3499	putative transcriptional regulatory protein, Crp/Fnr family	Regulatory (cNMP)	4.117	0.00
Mext_3500	UspA domain protein	Stress (universal)	3.573	0.00
Mext_3501	hypothetical protein	Translation (ribosomal conflict)	2.779	1.99E-260
Mext_3502	transport-associated	Transport	3.045	0.00
Mext_3503	hypothetical protein	Hypothetical	2.599	1.25E-148
Mext_3504	UspA domain protein	Stress (universal)	3.249	0.00
Mext_3505	regulatory protein Crp	Regulatory (cNMP)	3.699	0.00
Mext_3506	response regulator receiver	Regulatory	1.557	9.75E-27
Mext_3508	UspA domain protein	Stress (universal)	3.401	0.00
Mext_3509	metal-dependent phosphohydrolase HD sub domain	Signaling	2.707	2.11E-242
Mext_3523	hemolysin-type calcium-binding region	C-N hydrolase	-2.042	8.32E-29
Mext_3821	choloylglycine hydrolase	C-N hydrolase	2.101	1.03E-99
Mext_3833	cytochrome d ubiquinol oxidase, subunit II	Cytochrome metabolism	1.073	7.21E-17
Mext_3834	cytochrome bd ubiquinol oxidase subunit I	Cytochrome metabolism	1.358	2.35E-32
Mext_4099	ATP-binding region ATPase domain protein	Signaling	3.238	0.00
Mext_4100	carbonic anhydrase	pH	1.323	4.67E-28
Mext_4158	EfgA	Stress	-1.041	5.94E-35
Mext_4283	hypothetical protein	Hypothetical	1.306	6.29E-15
Mext_4421	hypothetical protein	Hypothetical	1.492	4.11E-24

Mext_4514	autoinducer-binding domain protein	Regulatory (quorum sensing)	1.280	2.40E-39
Mext_4556	heat shock protein Hsp20	Chaperone/heat shock	-1.055	8.33E-33
Mext_4599	flavin reductase domain protein FMN-binding	Redox rxn	1.809	8.86E-10
Mext_4618	nucleotide sugar dehydrogenase	Sugar metabolism	1.325	7.69E-05
Mext_4620	NAD-dependent epimerase/dehydratase	Sugar metabolism	1.145	6.81E-13
Mext_4700	integrase, catalytic region	Phage	-1.009	1.14E-05
Mext_4782	chaperonin GroEL	Chaperone/Heat shock	-1.477	6.20E-74
Mext_4783	chaperonin Cpn10	Chaperone/Heat shock	-1.385	4.09E-57

897 Table 2

898

Switch	Strain		Lag (hr)	Final Yield (Abs600)	p-value	Growth rate (μ)	p-value
S → M	WT		8	0.98 +/- 0.028		0.2139 +/- 0.002	
	Δ*ttmR*		14	0.84 +/- 0.014	0.090	0.2295 +/- 0.011	0.031
	Δ*efgA*		14	0.96 +/- 0.000	0.493	0.2077 +/- 0.001	0.575
M → S	WT		8	1.13 +/- 0.000		0.2333 +/- 0.018	
	Δ*ttmR*		8	1.13 +/- 0.000	0.500	0.2491 +/-0.003	0.471
	Δ*efgA*		8	1.12 +/- 0.014	NV	0.2325 +/- 0.018	0.960

899

900
901